

# Tumor Uptake and Metabolism of Copper-67-Labeled Monoclonal Antibody chCE7 in Nude Mice Bearing Neuroblastoma Xenografts

Ilse Novak-Hofer, Kurt Zimmermann, Helmuth R. Maecke, Hans Peter Amstutz, François Carrel and P. August Schubiger  
Paul Scherrer Institute, Radiopharmacy Division, Villigen; University Hospital, Department of Nuclear Medicine, Basel; and Swiss Red Cross, Central Laboratory of the Blood Transfusion Service, Bern, Switzerland

**Methods:** ChCE7, an internalizing, neuroblastoma-specific monoclonal antibody (MAb), and its F(ab')<sub>2</sub> fragments were derived with the bifunctional ligand 4-(1,4,8,11-tetraazacyclotetradec-1-yl)-methyl benzoic acid tetrahydrochloride (CPTA) and labeled with the potential therapeutic nuclide <sup>67</sup>Cu. After internalization and degradation of these immunoconjugates in SKN-AS human neuroblastoma cells, the terminal degradation product was found to be the lysine adduct of the copper complex. In vivo distributions in nude mice bearing neuroblastoma xenografts were studied and extracts from tumor and tissue samples were analyzed. **Results:** The intact MAb showed high tumor uptake, stable over 4 days postinjection (33.7% ± 2.8% ID/g), with tumor/blood ratios increasing from 4.4 on Day 1 to 23.0 on Day 7 postinjection and low levels of radioactivity in other tissues. Analysis of tumor extracts by gel filtration chromatography and high-pressure liquid chromatography (HPLC) showed that over the period of 4 days radioactivity was present both in a high M<sub>r</sub> form, consisting of the MAb/antigen complex, as well as in a low M<sub>r</sub> form, consisting of the copper complex attached to short peptides, including the lys-CPTA complex. There was no evidence of aggregates or MAb/antigen complexes in the blood, radioactivity being exclusively in the form of intact MAb, and radioactivity in the liver was found to consist of intact MAb, MAb fragments and the lys-CPTA metabolite. In the case of the F(ab')<sub>2</sub> fragments, high accumulation of radioactivity in the kidneys was observed and analysis of kidney extracts showed it to be due to rapid accumulation of the lys-CPTA complex. When kidney uptake and retention of the CPTA complex as well as of its lysine and glycine adducts was investigated, the lysine complex was taken up more strongly and retained longer in the kidneys than the other compounds. **Conclusion:** Copper-67-labeled MAb chCE7 F(ab')<sub>2</sub> fragments were prepared using a novel bifunctional copper ligand 1-(*p*-aminobenzyl)-1,4,7,10-tetraazacyclodecane-4,7,10-triacetate (DO3A). Compared with MAb-chCE7 F(ab')<sub>2</sub> fragments labeled by the CPTA ligand, labels using the DO3A ligand showed improved biodistributions resulting, 48 hr postinjection, in a 4-fold increase in tumor uptake and a 4-fold reduction of radioactivity in the kidneys.

**Key Words:** copper-67; antineuroblastoma antibody chCE7; radiolabeled antibody therapy; radiolabeled antibody metabolism

J Nucl Med 1997; 38:536-544

Neuroblastomas, embryonal tumors of the sympathetic nervous system occurring mainly in early childhood, can often be cured in Stages I to III, but their relapses (Stage IV disease) have poor prognosis with no more than 10% survival. Such relapses may appear as solid tumors, as bone marrow infiltrations or as a combination of both and become refractory to chemotherapy. Because only minor therapeutic success has been achieved in such cases, new therapeutic options have to be evaluated. Targeted immunotherapy using radiolabeled antineuroblastoma antibodies appears to be a promising alternative

because of its high tumor specificity. In particular, relapses, associated with bone marrow infiltrations, should aid radioimmunotherapy (RIT) because access of radioimmunoconjugates to disseminated tumor deposits is much better than to solid tumors. Indeed, excellent imaging of bone marrow metastasis has been achieved using radioiodinated antineuroblastoma monoclonal antibodies (MAbs) (1-3), and some therapeutic responses have been reported (1). MAb chCE7 is a chimeric antibody directed against a neuroblastoma-associated cell surface protein, which is internalized into its target cells (4-7). Clinical results with <sup>131</sup>I-chCE7 have shown that it is taken up rapidly and strongly into bone marrow infiltrations (2). Therefore, in such cases, we plan to use MAb chCE7 for RIT applications. For therapeutic applications it is thought that additional effectiveness may be achieved by choosing a therapeutic nuclide of more suitable radiation characteristics than the commonly used <sup>131</sup>I. In particular, reduced gamma emissions should reduce radiation burden to the patient and lower dose-limiting toxicity. The beta particle-emitting nuclide <sup>67</sup>Cu is a potential therapeutic nuclide with a mean beta emission energy of 141 keV, similar to <sup>131</sup>I but with a much reduced gamma component (182 keV, 42% compared with over 80% in the case of <sup>131</sup>I) and its half-life of 2.6 days is well suited to the biokinetics of antibodies.

We have previously examined internalization and degradation of <sup>67</sup>Cu-CPTA-chCE7 in SKN-AS human neuroblastoma cells and observed that radioactivity from <sup>67</sup>Cu-CPTA-chCE7 remains associated with its target cells for longer times than in the case of cells loaded with radioiodinated chCE7 (6). We found that cellular retention of a low M<sub>r</sub> <sup>67</sup>Cu-CPTA-chCE7 metabolite is the reason for this effect (6). In this study we found, using high-pressure liquid chromatography (HPLC) analysis, that the principal metabolite appearing in SKN-AS cells comigrated with the lysine adduct of the <sup>67</sup>Cu-CPTA complex and followed the appearance of low M<sub>r</sub> degradation products in tumors, livers and kidneys of nude mice bearing SKN-AS tumors after intravenous administration of intact and fragmented <sup>67</sup>Cu-CPTA-chCE7. Copper-67-chCE7 fragments were evaluated for RIT applications because they are thought to present advantages over intact MAbs due to their more rapid clearance from the blood and consequently their lower toxicity (8,9). We found high radioactivity levels in the kidney using <sup>67</sup>Cu-CPTA-chCE7 F(ab')<sub>2</sub> fragments, similar to results with other MAb F(ab')<sub>2</sub> fragments as reported by Smith et al. (9) and others (10,11). To delineate some factors contributing to this effect, we investigated in which form the radioactivity appears in the kidneys after injection of <sup>67</sup>Cu-CPTA-chCE7 F(ab')<sub>2</sub>. Because the principal metabolite we found consists of a lysine adduct of the copper complex, we asked if there is an influence of the terminal amino acid attached to the copper complex on radioactivity retained in kidneys. In addition, we tested a novel,

Received May 25, 1996; revision accepted Jul. 12, 1996.

For correspondence or reprints contact: P. August Schubiger, Paul Scherrer Institute, Radiopharmacy Division, CH-5232 Villigen-PSI, Switzerland.

more hydrophilic copper ligand to see what role the copper complex itself plays in kidney reuptake and retention of metabolites. The characterization of metabolism of  $^{67}\text{Cu}$ -chCE7 and its  $\text{F}(\text{ab}')_2$  fragments in nude mice bearing neuroblastoma xenografts provides the basis for their future clinical evaluation.

## MATERIALS AND METHODS

MAB chCE7 was purified from tissue culture supernatants by affinity chromatography with protein G Sepharose as described (7) and  $\text{F}(\text{ab}')_2$  fragments were made using a kit from Pierce (Pierce Europe B.V., The Netherlands) according to the manufacturer's protocol for human IgG1. Fragments were purified by fast protein liquid chromatography (FPLC) gel chromatography with Superose 6 and the purity of the preparations was checked with sodium dodecyl sulfate-polyacrylamide gel electrophoresis (SDS-PAGE).

The human neuroblastoma cell line SKN-AS was cultured as described (5) and was used for cell binding assays for quality control of labeled immunoconjugates, for generating subcutaneous tumors in nude mice and for studying cellular degradation of  $^{67}\text{Cu}$ -labeled immunoconjugates.

The bifunctional copper ligand 4-(1,4,8,11-tetraazacyclotetradec-1-yl)methyl benzoic acid tetrahydrochloride (CPTA) was custom synthesized according to the method of Studer et al. (12) and the bifunctional copper ligand 1-(*p*-nitrobenzyl)-1,4,7,10-tetraazacyclodecane-4,7,10-triacetate (DO3A) was synthesized according to (13).

**Synthesis of the Isothiocyanate Derivative of DO3A.** The DO3A ligand (5 mg) was dissolved in 1 ml of 3 M HCl. Thiophosgene (15  $\mu\text{l}$ , 97%) was added and the mixture was stirred overnight at room temperature in a sealed vial under  $\text{N}_2$ . The reaction mixture was then extracted with diethylether (2 ml) six times and dried in a Speed Vac. The dried product was suspended in 160  $\mu\text{l}$  of  $\text{H}_2\text{O}$ . The reaction was followed by HPLC [P18 column, 90%  $\text{H}_3\text{PO}_4$  (0.1%), 10% acetonitrile, 0.1 M ammonium acetate] and the product was characterized by mass spectroscopy.

## Synthesis of Lysine and Glycine Conjugates of CPTA

**1,8,11-Tert-butylloxycarbonyl-4-[(1,4,8,11-tetraazacyclotetradec-1-yl)methyl] Benzoic Acid ( $\text{BOC}_3\text{CPTA-OH}$ ).** To a suspension of 412 mg (842  $\mu\text{mol}$ )  $\text{CPTA} \cdot 4 \text{HCl} \cdot 0.5 \text{H}_2\text{O}$  in 20 ml of dioxane, 21 ml of 0.1 N NaOH were added resulting in a clear solution of pH  $\approx 12$ . At ice temperature, 715  $\mu\text{l}$  of di-tert-butyl-dicarbonate was added and the pH was kept around 12 by the addition of 1 N NaOH. After 6 hr, stirring the solvent was removed under reduced pressure below 40°C. The residue was dissolved in water and 1 M HCl was added to adjust the pH to 2. The aqueous solution was extracted three times with 10 ml ethyl acetate, the organic phase washed three times with 5 ml of saturated NaCl, dried over  $\text{Na}_2\text{SO}_4$ , filtered and evaporated on a rotary evaporator. The product was shown to be pure by thin-layer chromatography (TLC) ( $\text{SiO}_2/\text{CHCl}_3:\text{MeOH}:\text{NH}_3$  (conc.) = 2:2:1;  $R_f$  = 0.8). Yield: 413 mg (77.3%). FAB-MS:  $m/z$ : 635 ( $\text{M}+\text{H}^+$ ), 657 ( $\text{M}+\text{Na}^+$ ).  $^1\text{H}$  NMR ( $\text{CDCl}_3$ )  $\delta$ : 1.3–1.5 (m, 27H), 1.7 (s, broad, 2H), 1.9 (s, broad, 2H), 2.4 (s, broad, 2H), 2.65 (s, broad, 2H), 3.3–3.4 (m, broad, 12H), 3.6 (s, 2H), 7.4 (d, 2H), 8.05 (d, 2H).

**1,8,11-Tert-butylloxycarbonyl-4-[(1,4,8,11-tetraazacyclotetradec-1-yl)methyl] Benzoic Acid- $\epsilon$ -(BOC)-Lysine [ $\text{BOC}_3\text{-CPTA-}\epsilon$ -(BOC) Lys].** A solution of 250 mg (394  $\mu\text{mol}$ ) of  $\text{BOC}_3\text{CPTA-OH}$ , 127 mg of 1-hydroxy-7-azabenzotriazol and 67.5  $\mu\text{l}$  of diisopropylethylamine in 3 ml of dimethylformamide (DMF) was incubated for 10 min. Next, a solution of 97 mg of BOC-Lys-OH and 67.5  $\mu\text{l}$  of diisopropylethylamine in 2 ml of water was added and stirred for 5–10 min (TLC control). To this solution, 2 ml of 5%  $\text{NaHSO}_4$  and 7 ml of ethyl acetate were added. The aqueous phase was extracted twice with ethyl acetate and the ethyl acetate phases

washed three times with saturated NaCl. The combined ethyl acetate phases were dried over  $\text{Na}_2\text{SO}_4$ , filtered and evaporated on a rotary evaporator. The resulting oil solidified on the addition of ether. The product showed a minor impurity on TLC ( $\text{SiO}_2$ , chloroform: methanol = 1:1,  $R_f$  = 0.3). Yield: 260 mg (76.8%) FAB-MS:  $m/z$ : 863 ( $\text{M}+\text{H}^+$ ). A minor peak (TLC,  $R_f$  = 0.45) has  $m/z$  = 1091, which corresponds to di (BOC)-lysine adduct.

$^1\text{H}$  NMR ( $d_6$ -DMSO)  $\delta$ : 1.2–1.4 (m, 36H, BOC), 1.5–2.1 (m, 10H,  $\beta$ ,  $\gamma$ ,  $\delta$ - $\text{CH}_2$ -lys,  $-\text{CH}_2$ -), 3–3.8 (m, 18H,  $-\text{N-CH}_2$ -,  $\epsilon$ -lys), 3.85 (s, broad, 1H,  $\alpha$ -lys), 4.35 (s, broad, 2H, benzyl), 7.0 (d, 1H, NHBOC), 7.75 (d, 2H, arom), 7.9 (d, 2H, arom), 8.5 (s, broad, 1H, amide), 12.4 (s, very broad,  $-\text{COOH}$ ).

**Lysine[4-(1,4,8,11-tetraazacyclotetradec-1-yl)methyl] Benzoic Acid ( $\epsilon$ -Lys-CPTA).** Deprotection of  $\text{BOC}_3\text{-CPTA-}\epsilon(\text{BOC})\text{Lys}$  was afforded by the reaction of 100 mg of  $\text{BOC}_3\text{-CPTA-}\epsilon(\text{BOC})\text{Lys}$  in 0.5 ml of trifluoroacetic acid (TFA): $\text{H}_2\text{O}$ :thioanisole = 96:2:2 for 2 hr. The solvent mixture was evaporated and the product crystallized from acetone as a hygroscopic TFA salt.  $\epsilon$ -Lys-CPTA  $\cdot$  TFA was almost pure on TLC ( $\text{SiO}_2$ , isopropanol:  $\text{NH}_3$  = 7:3,  $R_f$  = 0.4) FAB-MS:  $m/z$  = 463 ( $\text{M}+\text{H}^+$ ) with a minor peak at 591 again corresponding to a little impurity from a dilysine adduct ( $R_f$  = 0.5). Yield: 66 mg (61.9%).

$^1\text{H}$  NMR ( $\text{D}_2\text{O}$ )  $\delta$ : 1.2–2.2 (m, 10H,  $\beta$ ,  $\gamma$ ,  $\delta$ - $\text{CH}_2$ -lys,  $-\text{CH}_2$ -), 2.9–3.5 (m, 18H,  $\text{NH-CH}_2$  = 16H  $\epsilon$ -lys- $\text{CH}_2$  = 2H), 3.55 (t, 1H,  $\alpha$ -lys- $\text{CH}$ -), 4.1 (s, 2H, benzyl), 7.5 (d, 2H, arom), 7.8 (d, 2H, arom).

**1,8,11-Tris(tert-butylloxycarbonyl)-4-[(1,4,8,11-tetraazacyclotetradec-1-yl)methyl] benzoic acid glycinamide ( $\text{BOC}_3\text{-CPTA-tBu-glycinate}$ ).**

A solution of 300 mg of  $\text{BOC}_3\text{CPTA-OH}$  (473  $\mu\text{mol}$ ), 152 mg of 1-hydroxy-7-azabenzotriazol and 162  $\mu\text{l}$  of diisopropylethylamine in 3 ml of DMF was incubated for 10 min at ambient. Afterwards, 87.2 mg of glycine-*t*-butylesterhydrochloride and 89  $\mu\text{l}$  of diisopropylethylamine in 2 ml of  $\text{H}_2\text{O}$  and 3 ml of DMF were added and stirred for 45 min.

$\text{BOC}_3\text{-CPTA-tBu-glycinate}$  was isolated as described for  $\text{BOC}_3\text{-CPTA-}\epsilon(\text{BOC})$ . Yield: 310 mg (87%) of FAB-MS:  $m/z$ : 749 ( $\text{M}+\text{H}^+$ ) [4-(1,4,8,11-tetraazacyclotetradec-1-yl)methyl] benzoic acid glycinamide (CPTA-gly). Deprotection was performed as described for  $\epsilon$ -Lys-CPTA. Yield: 86%. FAB-MS:  $m/z$ : 392.

$^1\text{H}$  NMR ( $\text{D}_2\text{O}$ )  $\delta$ : 1.8 (m, 2H,  $-\text{CH}_2\text{-CH}_2\text{-CH}_2-$ ), 2.1 (m, 2H,  $-\text{CH}_2\text{-CH}_2\text{-CH}_2-$ ), 2.75–3.35 (6 multiplets,  $\text{NH CH}_2$ ), 3.85 (s, broad, 2H,  $\text{CH}_2\text{-C}_6\text{H}_5$ ), 4.1 (s, 2H  $\text{N CH}_2$  COO), 7.42 (d, arom), 7.88 (d, arom).

Mass spectra were obtained on a V 670-SE mass spectrometer in a nitrobenzyl alcohol matrix at 8 keV. The  $^1\text{H}$ -NMR spectra were recorded at 360 MHz on a Bruker instrument in deuterated solvents using  $\text{Me}_4\text{Si}$  as internal standard.

## Radiolabeling

For  $^{67}\text{Cu}$  labeling by CPTA, MAB chCE7 and its  $\text{F}(\text{ab}')_2$  fragment were derived with the *N*-hydroxy-succinimide ester of the CPTA ligand as described (6). Purity of labeled preparations was checked by FPLC gel filtration chromatography over a Superose 6 column. Specific activities of  $^{67}\text{Cu}$ -CPTA immunoconjugates ranged between 0.5 and 1  $\mu\text{Ci}/\mu\text{g}$ .

For  $^{67}\text{Cu}$  labeling by the DO3A ligand activated ligand (10  $\mu\text{l}$ , 0.56  $\mu\text{mol}$ ) was added to 230  $\mu\text{l}$  of MAB chCE7  $\text{F}(\text{ab}')_2$  (2 mg, 0.02  $\mu\text{mol}$ ) in 0.1 M phosphate buffer (pH 8.0). The pH was raised to 9–10 by addition of 10  $\mu\text{l}$  of a saturated  $\text{Na}_3\text{PO}_4$  solution and incubated overnight at 4°C. Excess ligand was removed and a buffer change into 0.1 M citrate (pH 5.5) was effected using a centrifugation/dialysis device, and the immunoconjugate was stored at 4°C. For  $^{67}\text{Cu}$  labeling, 200  $\mu\text{g}$  of DO3A-chCE7  $\text{F}(\text{ab}')_2$  in 500  $\mu\text{l}$  of 0.1 M citrate buffer (pH 5.5) was incubated with 200

$\mu\text{Ci}$  of neutralized  $^{67}\text{Cu}$  (6) for 30 min at room temperature; EDTA was then added to a final concentration of 5 mM and incubation was continued for 5 min. The reaction mixture was purified over a G50 gel filtration column (10 cm  $\times$  0.5 cm) equilibrated in phosphate-buffered saline (PBS) or by FPLC over a Superose 6 column. Specific activity of  $^{67}\text{Cu}$ -DO3A-chCE7 F(ab')<sub>2</sub> ranged between 0.5 and 1  $\mu\text{Ci}/\mu\text{g}$ .

Immunoreactivity of radiocopper-labeled immunoconjugates was measured with a cell-binding assay using increasing numbers of SKN-AS cells dried to microtiter plates as described before (5) and was found to be 80–100% for the CPTA and DO3A conjugates.

TLC of  $^{67}\text{Cu}$ -labeled preparations was performed using silica gel plates and a solvent system consisting of 1 volume of methanol and 1 volume of 10% ammonium acetate according to Meares et al. (15). Autoradiography was with Amersham Hyperfilm MP at  $-80^\circ\text{C}$ , using Kodak intensifying screens.

Copper-67 activity was measured in a gamma counter using a 160- to 210-keV energy setting.

### Labeling of CPTA and CPTA Derivatives

Six hundred microliters of CPTA (1 mM), lysine-CPTA (1 mM) or glycine-CPTA (1 mM) in 0.1 M sodium acetate buffer (pH 5.5) were reacted for 30 min at ambient temperature with 2  $\mu\text{l}$  (126  $\mu\text{Ci}$ ) of  $^{67}\text{Cu}$ , which had been adjusted to pH 5.5 by the addition of sodium acetate buffer. After incubations, EDTA was added to a final concentration of 5 mM and samples were analyzed by TLC.

### Measurement of chCE7 Biodistributions in Tumor-Bearing Nude Mice

Adult female nude mice (strain ICR-ZH nu/nu) were used. Mice were injected subcutaneously with  $5 \times 10^6$  SKN-AS cells on each flank resulting, after 14–18 days, in tumors of 100–600 mg. Groups of three animals received injections of  $^{67}\text{Cu}$ -CPTA-chCE7 (5  $\mu\text{Ci}$ , 8  $\mu\text{g}$ ),  $^{67}\text{Cu}$ -CPTA-chCE7 F(ab')<sub>2</sub> fragments (5  $\mu\text{Ci}$ , 8  $\mu\text{g}$ ) or  $^{67}\text{Cu}$ -DO3A-chCE7 F(ab')<sub>2</sub> fragments (3  $\mu\text{Ci}$ , 10  $\mu\text{g}$ ) into the tail veins. At the indicated time points animals were killed and tumor, blood samples and the major organs were removed, rinsed in saline and counted in a gamma counter. The percent injected dose (%ID) was determined by measuring in parallel a diluted aliquot of the injected solutions. In some experiments, groups of three mice were injected with  $^{67}\text{Cu}$ -CPTA (0.5  $\mu\text{Ci}$ , 36 nmol),  $^{67}\text{Cu}$ -lys-CPTA (0.5  $\mu\text{Ci}$ , 35 nmol) and  $^{67}\text{Cu}$ -gly-CPTA (0.5  $\mu\text{Ci}$ , 24 nmol), and at the indicated times radioactivity was measured in blood, liver and kidney samples.

### Analysis of Tumor Cell Extracts

Internalization and degradation of  $^{67}\text{Cu}$ -chCE7 by SKN-AS cells was followed using an acid-elution endocytosis assay described previously (6). Briefly, SKN-AS cells ( $3 \times 10^6$  cells per 60-mm dish) were loaded with  $^{67}\text{Cu}$ -chCE7 (10  $\mu\text{g}/\text{dish}$ ) for 3.5 hr on ice and, after washing off, unbound MAb cells were incubated further for 20 hr at  $37^\circ\text{C}$  in a complete medium. Surface-bound MAb was then removed with an isotonic acidic buffer [0.1 M NaCl, 0.05 M glycine (pH 2.8)], cell layers were scraped into PBS, pelleted by a brief centrifugation step and lysed in a buffer consisting of 0.5% Nonidet P-40 (NP-40) in PBS, 1% iodoacetamide, 1 mM phenylmethylsulfonyl fluoride (PMSF), 50  $\mu\text{g}/\text{ml}$  aprotinin. Lysates were centrifuged for 5 min at full speed in a microcentrifuge and supernatants were subjected to HPLC or SDS-PAGE, followed by autoradiography.

### Analysis of Tissue Extracts

At the indicated time points after the injection of radiocopper-labeled immunoconjugates, tumor, liver, kidneys and blood were removed. Organs were briefly rinsed in ice-cold Tris-citrate buffer [0.1 M Tris-citrate (pH 6.5), 0.1 M NaCl] and homogenized with a

**TABLE 1**  
Uptake of Copper-67-CPTA-Labeled chCE7 in Neuroblastoma Xenografts over 7 Days

Tissue	Days				
	1	2	4	5	7
Tumor	33.5 $\pm$ 6.7	33.7 $\pm$ 10.3	33.7 $\pm$ 2.8	26.9 $\pm$ 9.9	11.5 $\pm$ 4.2
Blood	7.6 $\pm$ 1.6	5.0 $\pm$ 1.8	2.9 $\pm$ 0.5	2.0 $\pm$ 1.6	0.5 $\pm$ 0.2
Heart	2.7 $\pm$ 0.5	2.5 $\pm$ 1.1	1.3 $\pm$ 0.1	1.0 $\pm$ 0.5	0.7 $\pm$ 0.0
Liver	6.3 $\pm$ 0.9	5.2 $\pm$ 0.7	5.5 $\pm$ 1.6	3.3 $\pm$ 0.6	2.4 $\pm$ 0.6
Spleen	8.8 $\pm$ 3.0	9.4 $\pm$ 1.6	6.2 $\pm$ 1.6	6.1 $\pm$ 2.6	5.0 $\pm$ 1.3
Kidney	6.2 $\pm$ 0.0	5.7 $\pm$ 0.5	2.8 $\pm$ 1.9	3.5 $\pm$ 0.6	2.5 $\pm$ 0.6
Stomach	0.7 $\pm$ 0.3	1.1 $\pm$ 0.4	0.8 $\pm$ 0.2	0.5 $\pm$ 0.1	0.3 $\pm$ 0.1
Bowel	1.3 $\pm$ 0.3	1.6 $\pm$ 0.3	2.4 $\pm$ 2.2	0.7 $\pm$ 0.1	0.6 $\pm$ 0.2
Muscle	1.1 $\pm$ 0.3	0.9 $\pm$ 0.3	0.4 $\pm$ 0.3	0.5 $\pm$ 0.2	0.3 $\pm$ 0.1

Data are means  $\pm$  s.d. of three animals and are expressed in %ID/g tissue.

homogenizer in 5 ml/g extraction buffer consisting of Tris-citrate buffer including 0.5% NP-40, 1 mM PMSF, 50  $\mu\text{g}/\text{ml}$  aprotinin. Extracts were centrifuged for 20 min at  $45,000 \times g$  at  $4^\circ\text{C}$ , supernatants were filtered through a 0.45- $\mu\text{m}$  filter and separated by FPLC on a Superose 6-gel filtration column using PBS as solvent. Fractions (0.5 ml) were collected and counted in a gamma counter.

For HPLC analysis, EDTA was added to aliquots of tissue extracts to a final concentration of 5 mM; extracts were then precipitated with 30% ethanol for 15 min on ice, centrifuged for 5 min at maximal speed in a microfuge at  $4^\circ\text{C}$ , and the supernatants were concentrated using a concentrator. Up to 50  $\mu\text{l}$  of extracts were separated by reverse-phase HPLC, using an RP 18 column (5  $\mu\text{m}$ , 4 mm i.d.) and a solvent system consisting of 90% 0.1 M ammonium acetate in 0.1%  $\text{H}_3\text{PO}_4$  and 10% acetonitrile with a flow rate of 1 ml/min. Fractions (0.5 ml) were collected and radioactivity was measured in a gamma counter using an energy setting of 160–210 keV.

### Western Blot Analysis

Extracts from tumor xenografts and SKN-AS tumor cells were prepared using a Potter homogenizer in a buffer consisting of 0.1 M NaCl, 0.05 M Tris (pH 7.5), 0.5% NP 40, 1 mM PMSF, 50  $\mu\text{g}/\text{ml}$  aprotinin at a concentration of  $10^8$  cells/ml. Extracts were separated by 7.5% SDS-PAGE under nonreducing conditions, blotted onto nitrocellulose filters and the filters were probed with 100,000 cpm/ml  $^{125}\text{I}$ -chCE7 (4  $\mu\text{Ci}/\mu\text{g}$ ) according to the protocol provided by the manufacturer. Filters were exposed to Amersham MP film for 48 hr at  $-80^\circ\text{C}$  using Kodak intensifying screens.

## RESULTS

### Biodistribution of Copper-67-CPTA-chCE7 and Its F(ab')<sub>2</sub> Fragments in Tumor-Bearing Mice

Monoclonal antibody chCE7 was labeled with  $^{67}\text{Cu}$  as described in Methods and injected into the tail vein of nude mice bearing neuroblastoma (SKN-AS cells) xenografts. Table 1 shows biodistributions of  $^{67}\text{Cu}$ -chCE7 over a period of 7 days postinjection. Tumor uptake reached a maximum at Day 2 with 33.7% ID/g, remained high up to Day 5 and fell off between Day 5 and Day 7. High tumor/blood ratios were maintained over the whole period and kept increasing up to a maximal tumor/blood ratio of 23 at Day 7. Activity in liver, spleen and kidneys cleared more slowly than from blood; for example,

**TABLE 2**

Uptake of Copper-67-CPTA-Labeled chCE7 F(ab')<sub>2</sub> Fragments in Neuroblastoma Xenografts over 48 Hours

Tissue	Hours				
	4	8	12	24	48
Tumor	7.1 ± 2.3	9.0 ± 1.7	6.3 ± 2.0	5.5 ± 0.7	2.5 ± 0.9
Blood	1.7 ± 0.3	0.7 ± 0.1	0.5 ± 0.1	0.4 ± 0.0	0.4 ± 0.0
Heart	2.4 ± 0.8	1.8 ± 0.3	1.8 ± 0.2	1.5 ± 0.2	0.3 ± 0.1
Liver	6.0 ± 0.7	6.4 ± 2.0	6.8 ± 0.2	5.8 ± 0.7	5.5 ± 0.9
Spleen	6.6 ± 1.1	8.7 ± 5.4	8.4 ± 0.4	7.2 ± 1.1	4.9 ± 1.2
Kidney	138.2 ± 25.7	97.8 ± 5.7	107.6 ± 20.6	87.9 ± 8.4	60.0 ± 7.4
Stomach	0.4 ± 0.1	0.8 ± 0.1	0.6 ± 0.2	0.9 ± 0.2	1.0 ± 0.2
Bowel	0.9 ± 0.2	1.3 ± 0.4	1.3 ± 0.2	1.5 ± 0.2	1.3 ± 0.2
Muscle	0.5 ± 0.1	0.4 ± 0.1	0.4 ± 0.2	0.4 ± 0.1	0.3 ± 0.0

Data are means ± s.d. of three animals and are expressed in %ID/g tissue.

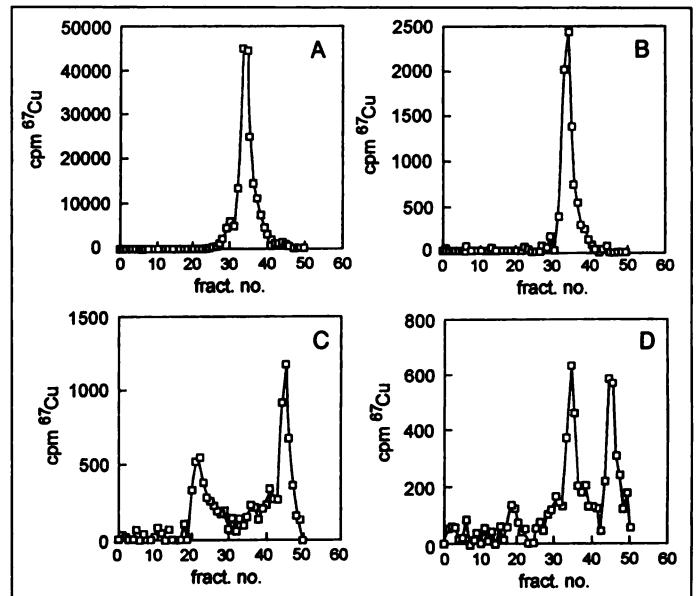
from 6.3% ID/g at Day 1 for liver to 2.4% ID/g at Day 7 and from 8.8% ID/g at Day 1 for spleen to 5.0% ID/g at Day 7.

When biodistributions of <sup>67</sup>Cu-chCE7 F(ab')<sub>2</sub> fragments were measured (Table 2) tumor uptake reached a peak after 8 hr with 9% ID/g. Activity was found to be clearing rapidly from blood with a tumor-to-blood ratio of 4 achieved 4 hr postinjection and a maximal tumor-to-blood ratio of 12.9 reached 8 hr postinjection. As in other systems (8,9), it was found that <sup>67</sup>Cu-chCE7 F(ab')<sub>2</sub> fragments showed high kidney uptake declining to 60% ID/g after 48 hr.

**Degradation Products of Intact and Fragmented Copper-67-chCE7**

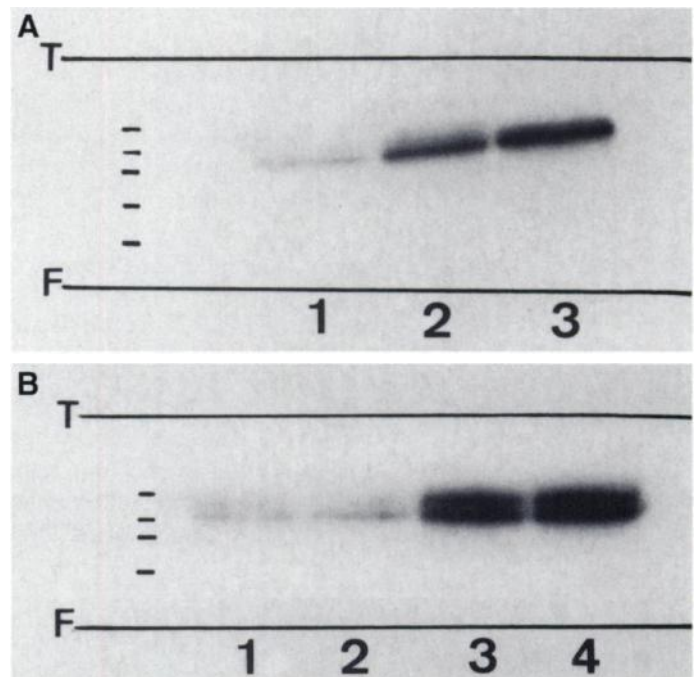
*Gel Filtration Analysis of Extracts from SKN-AS Tumor Xenografts, Liver and Blood After Injection of <sup>67</sup>Cu-chCE7 in Nude Mice.* To characterize radioactivity appearing in the blood, liver and neuroblastoma tumor xenografts at different times after injection of <sup>67</sup>Cu-chCE7, tissues were extracted and extracts were separated by gel filtration over a Superose 6 FPLC column. Gel filtration chromatography using this column will separate molecules in the M<sub>r</sub> range between 600 and 10 kDa and can distinguish between intact MAb, higher M<sub>r</sub> aggregates and fragments down to about 10 kDa. Lower M<sub>r</sub> metabolites will comigrate as a peak in fractions 42–52 at the end of the column.

Figure 1A shows the elution profile of intact <sup>67</sup>Cu-chCE7. Radioactivity present in the blood (Fig. 1B) one day postinjection essentially migrates to the position of the intact MAb. In contrast, extracts from tumors (Fig. 1C) show no peak at this position, radioactivity appearing instead in the form of a low M<sub>r</sub> peak (M<sub>r</sub> < 10,000) and in form of a high M<sub>r</sub> peak (M<sub>r</sub> > 670,000). Analysis of the high M<sub>r</sub> peak fraction by SDS-PAGE and Western blotting revealed the presence of both <sup>67</sup>Cu-chCE7 and the CE7-antigen (Fig. 2) indicating that this fraction contains antigen-antibody complexes. Gel filtration of liver extracts 1 day after injection of <sup>67</sup>Cu-chCE7 showed no evidence of a high M<sub>r</sub> peak, and radioactivity was found to be present both in the form of the intact antibody and of the low M<sub>r</sub> metabolites (Fig. 1D). Sometimes antibody fragments were also found to appear in liver extracts but were often difficult to resolve from the intact antibody peak. Table 3 summarizes results obtained from gel filtration analysis of tissue extracts 1 day and 2 and 4 days postinjection of <sup>67</sup>Cu-chCE7. Data are expressed as percent of radioactivity recovered in peak fractions, 100% being the amount of radioactivity when adding up all the fractions collected from the column. About 60%, in the



**FIGURE 1.** Separation of tissue extracts by gel filtration on Superose 6, 1 day postinjection of <sup>67</sup>Cu-chCE7: radioactivity profiles. (A) Control <sup>67</sup>Cu-chCE7, (B) serum, (C) tumor, (D) liver.

case of blood samples 80%, of the radioactivity is recovered in the indicated peaks, the rest being distributed as background over the column fractions. In blood the radioactivity remains essentially in the form of the intact antibody, whereas in tumor extracts a significant amount of radioactivity is present in the form of the low M<sub>r</sub> metabolites 1 day postinjection and radioactivity in this form keeps increasing over time. Tumor/liver ratios of <sup>67</sup>Cu-chCE7 vary between 5 (1 day postinjection) and 8 (5 days postinjection) (Table 3). When liver extracts are analyzed by gel filtration, one can also observe an increase in



**FIGURE 2.** Analysis of high molecular weight fraction after gel filtration of tumor extracts 1 day postinjection of <sup>67</sup>Cu-chCE7: Autoradiographs of an SDS-gel (A) and a Western blot probed with <sup>125</sup>I-chCE7 (B). (A) Track 1: tumor extract, tracks 2 and 3: control <sup>67</sup>Cu-chCE7. (B) Tracks 1 and 2: tumor extracts, tracks 3 and 4: extracts from SKN-AS cells. T = Top of gels and F = Dye front, lines show M<sub>r</sub> standards 200, 116, 97, 66 and 45 kDa from top to bottom.

**TABLE 3**  
Analysis of Tissue Extracts After Injection of Copper-67-chCE7: Gel Filtration on Superose 6

Peak fractions	Day 1			Day 2			Day 4		
	Blood	Tumor	Liver	Blood	Tumor	Liver	Blood	Tumor	Liver
High M <sub>r</sub> MAb	84.8 ± 1.2	21.9 ± 7.0	6.4 ± 2.2	82.5 ± 9.1	28.9 ± 4.3	4.0 ± 1.6	49.3 ± 6.8	10.2 ± 4.3	7.9 ± 2.4
MAb fragment		7.5 ± 5.2	8.6 ± 3.8		2.4 ± 0.5	19.3 ± 3.6			19.8 ± 5.4
Low M <sub>r</sub>		27.1 ± 11.6	25.0 ± 3.5		41.0 ± 5.2	29.6 ± 7.6		53.3 ± 14.0	43.4 ± 13.3

Data are means ± s.d. of three animals and are expressed in % radioactivity recovered in peak fractions, 100% being the sum of all the fractions collected.

radioactivity in form of the low M<sub>r</sub> metabolites over time, as in tumor extracts. However, the high M<sub>r</sub> MAb-antigen complex apparent in tumor extracts is found only at low levels in the liver and about 20% of the radioactivity is present in the form of intact MAb and MAb fragments.

#### HPLC Analysis of Low Molecular Weight Metabolites

We found previously that on internalization and degradation of <sup>67</sup>Cu-labeled MAb chCE7 by SKN-AS human neuroblastoma cells there is intracellular accumulation of a low M<sub>r</sub> metabolite (6). To define more closely this degradation product, extracts from SKN-AS cells in culture were analyzed after 20 hr of internalization and degradation of <sup>67</sup>Cu-chCE7 by reverse-phase HPLC (Fig. 3A, open squares). The CPTA ligand, as well as its lysine derivative, were labeled with <sup>67</sup>Cu and excess copper was chelated by EDTA, as described in Materials and Methods. A mixture of these standards was also chromatographed (Fig. 3A, closed triangles). Radioactivity present in the extracts was found to elute at the same fraction number as the lys-CPTA-<sup>67</sup>Cu standard, indicating that the principal metabolite appearing in SKN-AS cells during degradation of <sup>67</sup>Cu-chCE7 comigrates with the lysine adduct of the copper complex.

Gel filtration analysis of tumor and liver extracts after injection of <sup>67</sup>Cu-chCE7 into nude mice showed that 20%–30% of the recovered activity 24 hr postinjection is in the form of a low M<sub>r</sub> metabolite and that the amount of this metabolite increases over time (Table 3). It was found that the principal low M<sub>r</sub> metabolite comigrates with lys-CPTA-<sup>67</sup>Cu (Fig. 3B, C), both in tumor and liver extracts, when the extracts were analyzed by HPLC.

#### Metabolites in Kidney Extracts and Retention of Copper Complexes in the Kidney

Biodistributions of <sup>67</sup>Cu-labeled chCE7 F(ab')<sub>2</sub> fragments are characterized by high levels of radioactivity in the kidneys (Table 2). When kidney extracts were analyzed 2 hr after injection by HPLC most of the radioactivity was found to comigrate with the lys-CPTA copper complex.

It is unknown if the rapid accumulation of the lys-CPTA copper complex in the kidneys is due to the uptake of the metabolite into the kidney or due to retention of the metabolite generated within the proximal tubule cells of the kidney. High levels of radioactivity in the kidney are only observed with F(ab')<sub>2</sub> fragments and not with intact <sup>67</sup>Cu-chCE7 (Table 2). We investigated biodistributions of <sup>67</sup>Cu-CPTA, <sup>67</sup>Cu-lys-CPTA and <sup>67</sup>Cu-gly-CPTA in the blood, liver and kidneys of nude mice and found that the lys-CPTA copper complex is taken up more strongly and retained longer in the kidneys than either the CPTA-copper complex itself or its glycine adduct (Fig. 4). Blood levels of all three compounds were similar, whereas the gly-CPTA-copper complex accumulated somewhat more in the liver than did the lys-CPTA-copper complex (Table

4). These results support the hypothesis that the lys-CPTA-copper complex may have more efficient reuptake in the kidney than the CPTA complex itself or its glycine adduct.

#### Tumor Cell Retention and Kidney Accumulation of chCE7 and Its F(ab')<sub>2</sub> Fragments

To find out more about factors that contribute to the observed retention of low M<sub>r</sub> metabolites within tumor cells (Fig. 3) and in the kidneys of mice injected with <sup>67</sup>Cu-chCE7 F(ab')<sub>2</sub> fragments (Fig. 3), we labeled chCE7 with the DO3A ligand, a 4N-macrocyclic similar to CPTA but bearing three carboxylic groups. Figure 5 shows the chemical structures of the CPTA chelator (A) and the DO3A chelator (B) as well as a scheme of their conjugation to MAb chCE7 F(ab')<sub>2</sub>. When internalization and degradation of <sup>67</sup>Cu-DO3A-chCE7 was followed in SKN-AS cells, it was found that intracellular radioactivity accumulates and is retained to a similar extent to what we had found using <sup>67</sup>Cu-CPTA-chCE7. The results indicate that the presence of carboxylic groups on DO3A does not lead to a more rapid release of the terminal degradation product of <sup>67</sup>Cu-DO3A-chCE7 from tumor cells compared with the metabolite of the <sup>67</sup>Cu-CPTA-chCE7 (data not shown).

When chCE7 F(ab')<sub>2</sub> fragments were labeled with <sup>67</sup>Cu by the DO3A complex, injected into mice and radioactivity in various organs was measured at different times after injection, it was found that despite the large variability encountered at the earliest time after injection, radioactivity present in the kidney was reduced significantly (about 4 times less than with <sup>67</sup>Cu-CPTA-chCE7 F(ab')<sub>2</sub>) (Table 5). Other differences in biodistributions include a slower clearance from the blood and, possibly as a consequence of higher blood levels, at 48 hr postinjection, about 4-fold higher tumor levels with <sup>67</sup>Cu-DO3A-chCE7 F(ab')<sub>2</sub>.

#### DISCUSSION

The beta particle-emitting nuclide <sup>67</sup>Cu was originally selected as a potential therapeutic nuclide for RIT applications because of its favorable radiation characteristics and the availability of chelators that form copper complexes of high kinetic stability (6,12,16,17,18). We found previously that for the internalizing antineuroblastoma MAb chCE7, the degradation products of <sup>67</sup>Cu-labeled MAb chCE7 were retained intracellularly, which indicated that an additional therapeutic benefit might be achieved by the observed accumulations of <sup>67</sup>Cu-labeled metabolites in the target-tumor cells (6).

When tumor uptake of <sup>67</sup>Cu-chCE7 in nude mice bearing SKN-AS xenografts was measured it was found that radioactivity associated with tumor tissue remained at a high level for up to 5 days (Table 1). Compared with radioiodinated MAb chCE7 (5), biodistributions are characterized by prolonged retention of radioactivity in tumors, higher tumor-to-blood levels and higher levels (though not excessive) in liver and spleen, similar observations having been reported in other

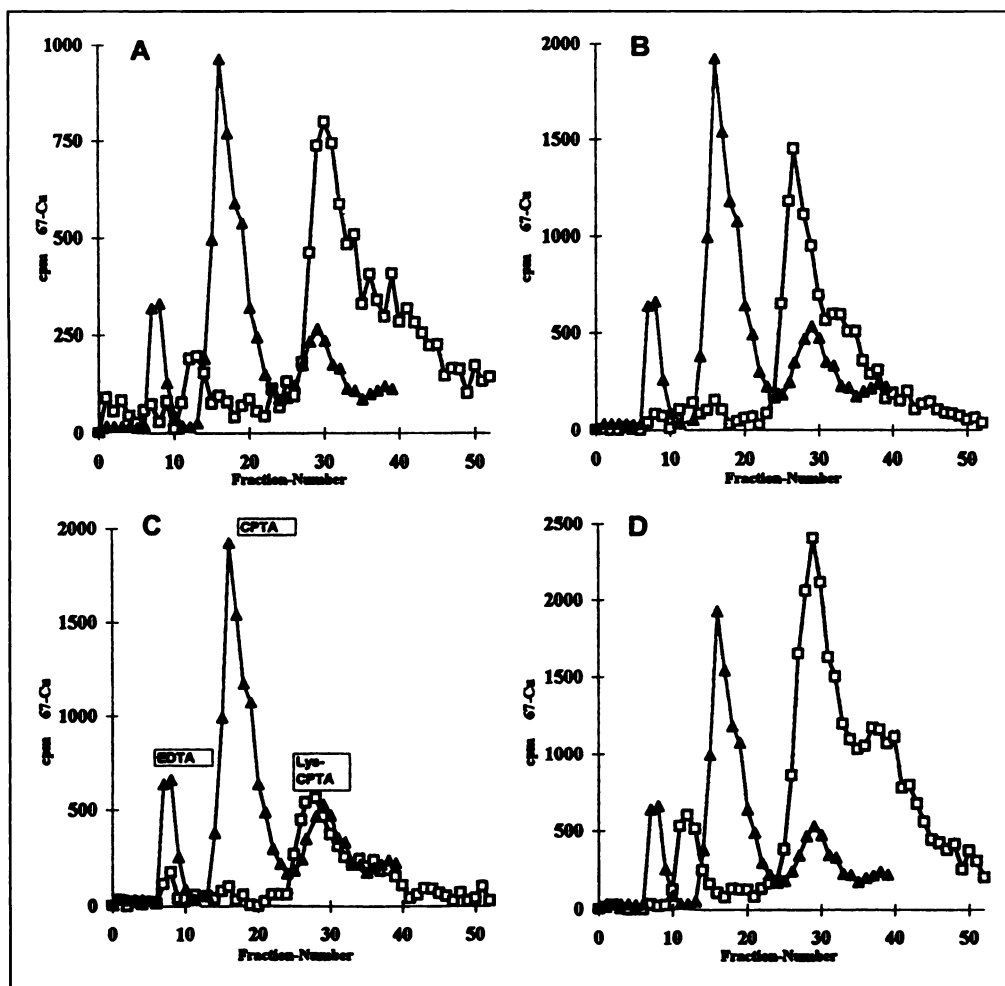


**FIGURE 3.** Separation of SKN-AS tumor cell extracts and tissue extracts by HPLC (open squares), 1 day (A, B, C) and 2 hr (D) after application of  $^{67}\text{Cu}$ -chCE7. The trace with triangles represents a mixture of the  $^{67}\text{Cu}$  complexes with EDTA (fraction No. 8), CPTA (fraction No. 16) and lys-CPTA (fraction No. 29). (A) Tumor cells, (B) tumor xenografts, (C) liver, (D) kidney.

systems (9,16). To find out more about the reasons for these differences in biodistributions between radioiodinated and radiocopper-labeled MAbs, radioactivity present in tumor extracts was analyzed by gel filtration chromatography. It was found that, as early as 1 day postinjection, a significant proportion of the radioactivity is present in the form of low  $M_r$  metabolites and that at Day 4 postinjection, when tumor levels are still high, about 50% of the radioactivity is of low  $M_r$  (Fig. 2, Table 3). These results indicate that our earlier observation on the tumor cell retention of low  $M_r$   $^{67}\text{Cu}$ -labeled MAb metabolites (6) and washout of iodotyrosine, in the case of radioiodinated MAb chCE7 (4), made in the in vitro cell culture system extends to the in vivo situation. Analysis of SKN-AS cell extracts after 20 hr of internalization and degradation of  $^{67}\text{Cu}$ -chCE7 by TLC (data not shown) and by HPLC (Fig. 3) show that most of the intracellular radioactivity comigrates with the lysine adduct of the  $^{67}\text{Cu}$ -CPTA complex (Fig. 3), supporting the idea that the copper-labeled MAb is degraded in lysosomes by proteases into peptide fragments, with the terminal degradation product being the copper complex attached to the lysine residues, over which derivatization of the CPTA ligand to the MAb is performed. Similar conclusions were reached by Franano et al. (19) based on results with endocytosed  $^{111}\text{In}$ -DTPA-labeled glycoproteins, where the terminal degradation product was found to be  $^{111}\text{In}$ -DTPA-lysine. The low  $M_r$  peak appearing in tumor and liver extracts was also

found to comigrate with the lys-CPTA- $^{67}\text{Cu}$  metabolite. A complete proof of identity of the low  $M_r$  metabolite probably could be achieved only by mass spectroscopy. Analysis of tumor extracts shows, in addition to the presence of low  $M_r$ ,

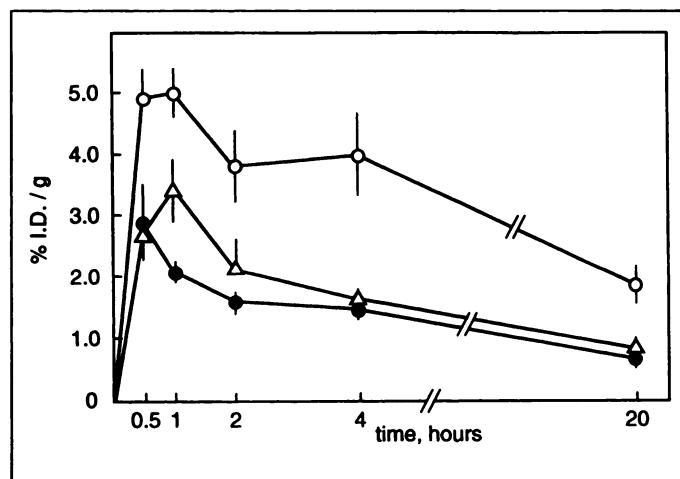


**FIGURE 4.** Radioactivity measured in kidneys after injection of  $^{67}\text{Cu}$ -labeled complexes into nude mice. Open circles =  $^{67}\text{Cu}$ -lys-CPTA; open triangles =  $^{67}\text{Cu}$ -gly-CPTA; closed circles =  $^{67}\text{Cu}$ -CPTA. Results are means  $\pm$  s.e.m. of two experiments performed with groups of three mice and are expressed as % ID/g kidney.

**TABLE 4**

Biodistribution of Copper-67-CPTA, Lys-CPTA and Gly-CPTA in Nude Mice over 20 Hours

Hours	Tissues	CPTA	Lys-CPTA	Gly-CPTA
0.5	Blood	0.76 ± 0.33	0.75 ± 0.14	0.33 ± 0.01
	Kidney	2.88 ± 0.70	4.85 ± 0.54	2.67 ± 0.24
	Liver	n.d.	0.96 ± 0.16	2.28 ± 0.63
1.0	Blood	0.20 ± 0.04	0.41 ± 0.22	0.07 ± 0.04
	Kidney	2.07 ± 0.13	4.98 ± 0.40	3.43 ± 0.57
	Liver	n.d.	0.94 ± 0.15	1.18 ± 0.55
2.0	Blood	0.06 ± 0.03	0.07 ± 0.02	0.13 ± 0.01
	Kidney	1.63 ± 0.04	3.76 ± 0.57	2.12 ± 0.48
	Liver	n.d.	0.90 ± 0.19	2.56 ± 0.28
4.0	Blood	0.06 ± 0.01	0.07 ± 0.01	0.12 ± 0.02
	Kidney	1.48 ± 0.15	3.97 ± 0.74	1.57 ± 0.07
	Liver	n.d.	0.88 ± 0.03	2.13 ± 0.25
20.0	Blood	0.05 ± 0.01	0.07 ± 0.00	0.12 ± 0.00
	Kidney	0.65 ± 0.07	1.92 ± 0.29	0.78 ± 0.07
	Liver	n.d.	0.72 ± 0.09	1.02 ± 0.00

Data are means ± s.d. of three animals and are expressed in % ID/g tissue. n.d. = not determined.

metabolites, radioactivity in form of a high  $M_r$  peak (Fig. 2, Table 3). When the high  $M_r$  fraction was analyzed by SDS-PAGE and by Western blotting it was found to contain the chCE7 antigen as well as intact  $^{67}\text{Cu}$ -labeled MAb chCE7 (Fig. 2), indicating that the fraction consists of antigen/MAB complexes. Such complexes are present in tumor tissue for at least 4 days postinjection, which probably reflects a continuous supply of  $^{67}\text{Cu}$ -chCE7 to the tumor and indicates that, in the case of this internalizing MAB and despite internalization and degradation, MAB remains associated with tumor tissue for extended periods of time. The radioactivity in the blood was found to be in the form of the intact MAB, appearing at the same position as control  $^{67}\text{Cu}$ -chCE7 (Fig. 1, Table 3), showing that there are no aggregates or antigen/MAB complexes circulating in the blood as in the case of other systems, which could lead to

**TABLE 5**

Uptake of Copper-67-DO3A-Labeled chCE7 F(ab')<sub>2</sub> Fragments in Neuroblastoma Xenografts over 48 Hours

Tissue	Hours			
	4	8	24	48
Tumor	8.8 ± 1.3	11.4 ± 2.0	8.9 ± 2.4	10.2 ± 1.9
Blood	18.1 ± 0.8	8.7 ± 1.3	1.4 ± 0.6	0.8 ± 0.1
Heart	8.2 ± 1.9	4.8 ± 0.4	2.6 ± 0.3	2.1 ± 0.3
Liver	10.1 ± 0.9	10.3 ± 0.4	11.4 ± 3.2	7.5 ± 0.7
Spleen	7.0 ± 1.7	6.2 ± 1.0	5.3 ± 0.1	3.6 ± 0.2
Kidney	32.5 ± 4.9	30.5 ± 0.4	21.5 ± 0.5	14.1 ± 3.0
Stomach	1.0 ± 0.2	1.3 ± 0.6	0.5 ± 0.2	0.5 ± 0.1
Bowel	2.2 ± 0.4	2.0 ± 0.5	1.5 ± 0.4	1.7 ± 0.1
Muscle	1.5 ± 0.2	1.1 ± 0.1	0.8 ± 0.2	0.7 ± 0.0

Data are means ± s.d. of three animals and are expressed as percent injected dose per gram of tissue.

unwanted increased uptake into the reticuloendothelial system and especially in the liver (20).

When analyzing liver extracts there was no evidence of significant levels of high  $M_r$  antigen-MAB complexes, radioactivity appearing instead in the form of intact undegraded  $^{67}\text{Cu}$ -chCE7, of smaller  $M_r$  fragments and in the form of the lys-CPTA- $^{67}\text{Cu}$  metabolites (Figs. 1, 3, Table 3). Low  $M_r$   $^{67}\text{Cu}$ -chCE7 metabolites accumulate in the liver as in the tumor, the absolute levels in the liver, however, are more than five times lower (Table 1). It remains to be seen if accumulation of  $^{67}\text{Cu}$ -labeled MAB metabolites in the liver will present problems in the clinical situation. In this context, the possibility of PET imaging with  $^{64}\text{Cu}$ -labeled chCE7 represents another advantage of the copper isotopes, since it will permit studies on the doses delivered to tumor and liver or other critical organs, allowing individualized treatment planning (10,21).

The problem of unwanted tissue accumulation encountered with radiometal-labeled immunoconjugates has been evident especially with MAB fragments (9-11). In the case of F(ab')<sub>2</sub> fragments labeled with radiocopper by the CPTA ligand, activity was reported to accumulate in the kidneys (9,10). When  $^{67}\text{Cu}$ -CPTA-labeled chCE7 F(ab')<sub>2</sub> fragments were investigated, we also found high levels of radioactivity in the kidneys (Table 2). Analysis of kidney extracts by HPLC revealed that at 2 hr postinjection most of the radioactivity already appeared in form of the lys-CPTA metabolite (Fig. 3). There was no evidence that the  $^{67}\text{Cu}$ -CPTA complex is unstable, because after addition of EDTA to extracts to complex "loosely" bound copper, no  $^{67}\text{Cu}$ -EDTA was found (Fig. 3). The data suggest that  $^{67}\text{Cu}$ -CPTA-F(ab')<sub>2</sub> fragments or F(ab) fragments, which may be generated from the F(ab')<sub>2</sub> elsewhere and enter the kidney, are rapidly degraded and the lys-CPTA complex is subject to reuptake. It has been hypothesized that the interchain disulfide bond of F(ab')<sub>2</sub> fragments is readily cleaved in vivo (22) and we, therefore, investigated if Cu-CPTA-chCE7 F(ab')<sub>2</sub> fragments are degraded more rapidly in SKN-AS tumor cells than intact  $^{67}\text{Cu}$ -CPTA-chCE7. Although we did not find significant differences in the rate of lysosomal degradation (data not shown), this does not exclude that in the compartment in which the  $^{67}\text{Cu}$ -CPTA-chCE7-fragment enters the body there are different conditions favoring rapid degradation. We found that the terminal amino acid attached to the copper-CPTA complex plays a role in its kidney retention because lys-CPTA

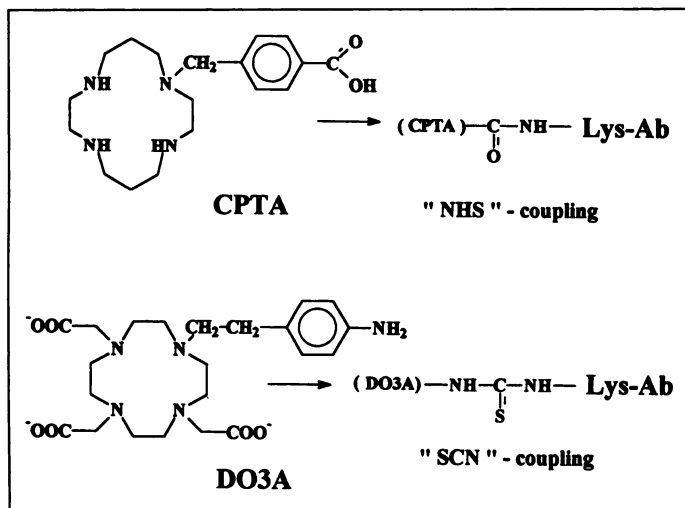


**FIGURE 5.** Chemical structures of the bifunctional copper chelators (A) CPTA and (B) DO3A. "NHS," coupling of *n*-hydroxysuccinimide ester of CPTA to lysine residues of Ab. "SCN," coupling of isothiocyanate derivative of DO3A to lysine residues of Ab.

was found to be taken up to a larger extent and retained longer than either the CPTA complex by itself or its glycine adduct (Fig. 4, Table 4). Similarly, increased renal accumulation was observed (19) after intravenous injection of  $^{111}\text{In}$ -DTPA-lysine compared with  $^{111}\text{In}$ -DTPA. It has been hypothesized that basic amino acids may be adsorbed more strongly into the negatively-charged cell membranes of proximal tubule cells. Our results suggest that a search for derivatization methods, which would avoid the formation of terminal degradation products bearing basic amino acid residues such as lysine, may lead to radio-metal-labeled antibody fragments showing less accumulation of radioactivity in the kidneys. One way of achieving this is by introducing peptide linkers between metal chelates and MABs containing protease sensitive sequences. Linkers such as ala-leu-ala-leu or (gly) $_3$ -L-phe, being potential substrates for lysosomal proteases, have been investigated (23–25) and were found to improve biodistribution in some instances (25).

Because charge and hydrophilicity of the copper complex itself should also influence its cellular retention as well as its reuptake, we tested biodistributions of chCE7-F(ab') $_2$  fragments labeled with a carboxylated 12N4 macrocycle (DO3A). Similar ligands such as the 14N4 carboxylated TETA ligand had already been used successfully for copper labeling of MABs and their F(ab') $_2$  fragments (11,17,26) and it had been reported that such preparations show less kidney uptake than copper-CPTA-labeled F(ab') $_2$  fragments (11,26,27). The DO3A complex we use is anionic in contrast to the cationic CPTA complex and more hydrophilic. It is coupled to lysine residues of MAB chCE7 using the isothiocyanate method and appears as a single peak on FPLC with no evidence of contaminating labeled fragments. Using this ligand, kidney uptake of chCE7-F(ab') $_2$  fragments was found to be reduced about 4-fold compared with the CPTA ligand, achieving similar levels (14.1%  $\pm$  3.0% ID/g) 48 hr postinjection to those reported by Anderson et al. (27) for the  $^{64}\text{Cu}$  BAT-2IT-1A3-F(ab') $_2$  fragment in rats. Tumor uptake of  $^{67}\text{Cu}$ -DO3A-chCE7 F(ab') $_2$  fragments is characterized by a prolonged retention in tumor compared with the  $^{67}\text{Cu}$ -CPTA-chCE7, resulting in 4-fold higher levels in the tumor 48 hr postinjection. Despite these improvements, it appears that therapeutic doses of  $^{67}\text{Cu}$ -DO3A-chCE7 F(ab') $_2$  would still result in an unacceptably high radiation burden to the kidneys. However, from dosimetry calculations based on PET images as elaborated by Anderson et al. (27), doses delivered to the kidney are acceptable for diagnostic imaging.

When we compared the rates of intracellular degradation of  $^{67}\text{Cu}$ -CPTA-chCE7 F(ab') $_2$  and  $^{67}\text{Cu}$ -DO3A-chCE7 F(ab') $_2$  and cellular accumulation of their terminal degradation products in SKN-AS cells, we did not find any striking differences that would explain their in vivo behavior. These results suggest that the differences observed in vivo of the two immunoconjugates we studied may reside not as much in their rates of intracellular degradation, accumulation and release of metabolites, but rather in a different behavior of metabolites once they are released from the cells where degradation takes place. Clearly, more insight into the factors that influence clearance of peptide- or amino acid-linked metal complexes from tissues will be important for the design of improved radioimmunoconjugates.

Concerning intact  $^{67}\text{Cu}$ -chCE7, we found that in contrast to radioiodinated chCE7, which shows high uptake into neuroblastoma xenografts up to 2 days postinjection (5),  $^{67}\text{Cu}$ -chCE7 is present in tumor tissue at high levels up to 5 days postinjection, both in the form of MAB-antigen complex and low  $M_r$  metabolites. This property together with the low levels found in other

tissues and the more favorable radiation characteristics of  $^{67}\text{Cu}$  compared with  $^{131}\text{I}$  make it a potentially effective therapeutic agent.

## ACKNOWLEDGMENTS

We thank Dr. A. Smith for helpful discussions and Ms. C. Ruch, P. Powell and F. Evard for excellent technical help and Ms. H. Christen for expert secretarial assistance. We also thank "Nachlass Frau Dr. Steiger," Mallinckrodt, Inc. and the Swiss National Science Foundation (Project No. 31-32586.91) for financial support.

## REFERENCES

- Cheung NK, Yeh SDJ, Gulati S, et al. Iodine-131-3F8 targeted radiotherapy of neuroblastoma: a phase I clinical trial. *Proc Am Assoc Cancer Res* 1990;31:284.
- Doerr U, Haldemann AR, Leibundgut K, et al. First clinical results with the chimeric antibody chCE7 in neuroblastoma: targeting features and biodistribution data [Abstract]. *Eur J Nucl Med* 1993;20:858.
- Yeh SDJ, Larson SM, Burch L, et al. Radioimmunodetection of neuroblastoma with iodine-131-3F8: correlation with biopsy, iodine-131-meta iodobenzylguanidine and standard diagnostic modalities. *J Nucl Med* 1990;32:769–776.
- Novak-Hofer I, Amstutz H, Morgenthaler JJ, et al. Internalization and degradation of monoclonal antibody chCE7 by human neuroblastoma cells. *Int J Cancer* 1994;57:427–432.
- Novak-Hofer I, Amstutz H, Haldemann A, et al. Radioimmunolocalization of neuroblastoma xenografts with chimeric antibody chCE7. *J Nucl Med* 1992;33:231–236.
- Novak-Hofer I, Amstutz H, Mäcke HR, et al. Cellular processing of copper-67-labeled monoclonal antibody chCE7 by human neuroblastoma cells. *Cancer Res* 1995;55:46–50.
- Amstutz H, Rytz CH, Novak-Hofer I, et al. Production and characterization of mouse/human chimeric antibody directed against human neuroblastoma. *Int J Cancer* 1993;53:137–152.
- Buchegger F, Pelegrin A, Delaloye B, et al. Iodine-131-labeled MAB F(ab') $_2$  fragments are more efficient and less toxic than intact anti-CEA antibodies in radioimmunotherapy of large human colon carcinoma grafted in nude mice. *J Nucl Med* 1990;31:1035–1044.
- Smith A, Alberto R, Bläuenstein P, et al. Preclinical evaluation of  $^{67}\text{Cu}$ -labeled intact and fragmented anti-colon carcinoma monoclonal antibody MAB35. *Cancer Res* 1993;53:5727–5733.
- Anderson CJ, Connert JM, Schwarz SW, et al. Copper-64-labeled antibodies for PET imaging. *J Nucl Med* 1992;33:1685–1691.
- Mausner LF, Srivastava SC, Kolsky KL, et al. Development and evaluation of copper-67 labeled DOTA and TETA immunoconjugates for radioimmunotherapy [Abstract]. *J Labelled Compounds Radiopharm* 1994;35:374–376.
- Studer M, Kaden TA, Mäcke HR. Metal complexes with macrocyclic ligands: reactivity studies of the pendant carboxylic group in a macrocyclic Cu $^{2+}$  complex towards amide formation and its use as a protein-labeling agent. *Helv Chim Acta* 1990;73:149–153.
- Ruser G, Ritter W, Mäcke HR. Synthesis and evaluation of two new bifunctional carboxymethylated tetraazamacrocyclic chelating agents for protein labeling with indium-111. *Bioconj Chem* 1990;2:345–349.
- Schwarzbach R, Zimmermann K, Bläuenstein P, et al. Development of a simple and selective separation of  $^{67}\text{Cu}$  from irradiated zinc for use in antibody labeling: a comparison of methods. *Appl Radiat Isot* 1995;46:329–336.
- Meares CF, McCall MJ, Reardon DT, et al. Conjugation of antibodies with bifunctional chelating agents: isothiocyanate and bromoacetamide reagents, methods of analysis and subsequent addition of metal ions. *Anal Biochem* 1984;142:68–78.
- Smith-Jones PM, Fridrich R, Kaden TA, et al. Antibody labeling with copper-67 using the bifunctional macrocycle 4-[1,4,8,11-tetraazacyclotetradec-1-yl-methyl] benzoic acid. *Bioconj Chem* 1991;2:415–421.
- Deshpande SV, DeNardo SJ, Meares CF, et al. Copper-67 labeled monoclonal antibody Lym-1, a potential radiopharmaceutical for cancer therapy: labeling and biodistribution in RAJI tumored mice. *J Nucl Med* 1988;29:217–225.
- De Nardo GL, De Nardo SJ, Meares CF, et al. Pharmacokinetics of copper-67 conjugates Lym-1, a potential therapeutic radioimmunoconjugate in mice and in patients with lymphoma. *Antib Immunoconj Radiopharm* 1991;4:777–785.
- Franano FN, Edwards WB, Welch MJ, et al. Metabolism of receptor targeted  $^{111}\text{In}$ -DTPA-glycoproteins: identification of  $^{111}\text{In}$ -DTPA- $\epsilon$ -lysine as the primary metabolic and excretory product. *Nucl Med Biol* 1994;5:1023–1034.
- Pimm MV. Circulating antigen: bad or good for immunoscintigraphy? *Nucl Med Biol* 1995;22:137–145.
- Larson SM, Pentlow KS, Volkow ND, et al. PET scanning of iodine-124-3F9 as an approach to tumor dosimetry during treatment planning for radioimmunotherapy in a child with neuroblastoma. *J Nucl Med* 1992;33:2020–2023.
- Siddiqui A, Quadri SM, Griffith GL, et al. Tumor targeting and pharmacokinetics of unmodified and modified F(ab) $_2$  fragments of an anti-CEA murine monoclonal antibody (immuno-14). *Nucl Med Biol* 1995;4:425–435.
- Studer M, Kroger LA, De Nardo SJ, et al. Influence of a peptide linker on biodistribution and metabolism of antibody-conjugates benzyl-EDTA: comparison of enzymatic digestion in vitro and in vivo. *Bioconj Chem* 1992;3:424–429.

24. Li M, Mearns CF. Synthesis, metal chelate stability studies and enzyme digestion of a peptide-linked DOTA derivative and its corresponding radiolabeled immunoconjugates. *Bioconj Chem* 1993;4:275-283.
25. De Nardo SJ, Zhong G-R, Salako Q, et al. Pharmacokinetics of chimeric L6 conjugated to indium-111 and yttrium-90-DOTA-peptide in tumor-bearing mice. *J Nucl Med* 1995;36:829-836.
26. Anderson CJ, Rogers BE, Connett JM. Comparison of two bifunctional chelates for labeling  $^{64}\text{Cu}$  to MAb 1A3 and 1A3 F(ab')<sub>2</sub>: chemistry and animal biodistribution [Abstract]. *J Labelled Compounds Radiopharm* 1994;35:313-315.
27. Anderson CJ, Schwarz SW, Connett JM, et al. Preparation, biodistribution and dosimetry of Copper-64-labeled anti-colorectal carcinoma monoclonal antibody fragments 1A3 F(ab')<sub>2</sub>. *J Nucl Med* 1995;36:850-858.

(continued from page 5A)

## FIRST IMPRESSIONS

### GI Bleeding?

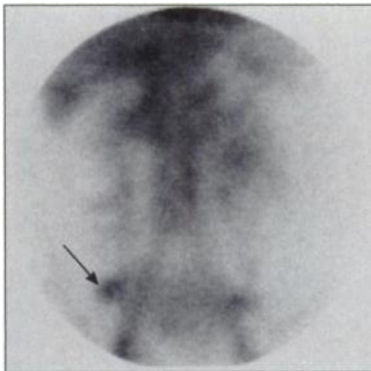


**Figure 1.**

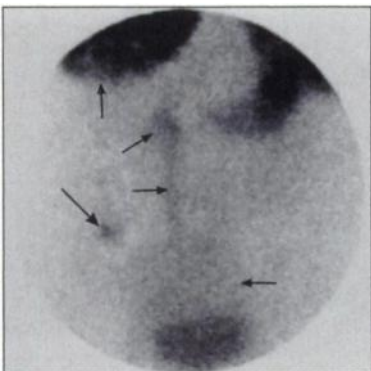


**Figure 2.**

### PURPOSE

A 26-yr-old female was investigated for gastrointestinal (GI) bleeding after a low uterine segment cesarean section. A GI bleeding study with  $^{99\text{m}}\text{Tc}$ -labeled red blood cells (Fig. 1) demonstrated a bleeding focus on the fourth postoperative day in the right lower quadrant. Technetium-99m-pertechnetate imaging (Fig. 2) clearly demonstrated an abnormal focus corresponding to the GI bleed study abnormality in the right lower quadrant. This was subsequently resected and demonstrated to be a Meckel's diverticulum (large arrow). Gastric activity is also seen. The pertechnetate study reveals evidence of the recent pregnancy with a dilated right renal pelvis and ureter, prominent uptake in lactating breasts and blood pool in an enlarged postpartum uterus (small arrows).

### TRACER

Technetium-99m-pertechnetate (as sodium pertechnetate), 370 MBq (10 mCi)

### ROUTE OF ADMINISTRATION

Intravenous

### TIME AFTER INJECTION

Immediate flow/dynamic study with 1-minute frames thereafter for 30 minutes

### INSTRUMENTATION

Large field of view gamma camera with a low-energy, high-resolution parallel-hole collimator

### CONTRIBUTORS

Stephen L. Stuckey, St. Vincent's Hospital and Peter MacCallum Cancer Institute, Melbourne, Australia.